Acta of Bioengineering and Biomechanics
Vol. 14, No. 3, 2012

Original paper
DOI: 10.5277/abb120307

Numerical modelling and verification of Polish ventricular assist device

ANDRZEJ MILENIN[1], MAGDALENA KOPERNIK[1]*, DOROTA JURKOJĆ[2], MACIEJ GAWLIKOWSKI[2], TOMASZ RUSIN[3], MACIEJ DARŁAK[2], ROMAN KUSTOSZ[1,2]

[1] AGH University of Science and Technology, Kraków, Poland.
[2] Foundation of Cardiac Surgery Development, Zabrze, Poland.
[3] Elhys Sp. z o.o., Warszawa, Poland.

The developed multiscale model of blood chamber of POLVAD (Polish ventricular assist device) was introduced. The tension test for polymer and digital image correlation (DIC) were performed for verification of the strains and displacements obtained in the numerical model of POLVAD_EXT. The numerical simulations were carried out in conditions given in the experiment to compare the results obtained on external surfaces of blood chamber of the POLVAD_EXT. The examined polymer applied in the POLVADs is sensitive to changes of temperature and this observation is considered in all prepared numerical models. The comparison of experimental and numerical results shows acceptable coincidence. There are some heterogeneous distributions of strains in experiment with respect to analysis of computed parameters. The comparison of two versions of blood chambers (POLVAD and POLVAD_EXT) in numerical analysis shows that POLVAD_EXT construction is better with respect to analysis of strain and stress. The maximum values of computed parameters are located in the regions between connectors on the internal surfaces of blood chambers of POLVAD.

Key words: *finite element method (FEM), representative volume element (RVE), titanium nitride (TiN), ventricular assist device (VAD), digital image correlation (DIC), polymer*

1. Introduction

In the "Polish Artificial Heart Programme 2007–2011" [13] efforts are made towards development of such a pump of Polish ventricular assist device (POLVAD) that is low energy consuming and does not cause red blood cell trauma, as well as such a construction of POLVAD that is durable, biocompatible and allows monitoring. The walls of the proposed design of POLVAD are made of polymer and are supposed to be covered with a titanium nitride (TiN) nanocoating to improve the haemocompatibility [1] and properties of the surface of the medical device.

Similar constructions of pneumatic and polymeric ventricular assist devices are [4]: Abiomed AB5000 (USA), Thoratec PVAD (USA), Berlin Heart EXCOR (Germany) and Medos HIA-VAD (Germany). The above-mentioned VADs are not coated and the Polish proposition of VAD is closest to the construction of Medos. Published works dedicated to the VAD issue are focused on a numerical research. However, they lead only to a blood flow characteristics in macro- [2] and in microscales [12], [14]. Summarizing, there are no physical and numerical models of such an exact multilayer construction of POLVAD_EXT in the world literature, because the presented construction of VAD is Polish proposal. Thus, the authors based their work on the state of art and on literature of Polish authors.

The first step in Polish mechanical circulatory support was made by Professor Religa in 1993, who implanted the POLVAD. The second version of POLVAD

* Corresponding author: Magdalena Kopernik, AGH University of Science and Technology, al. Mickiewicza 30, 30-059 Kraków, Poland. Tel.: +48 12 6173866, fax.: +48 12 6172921, e-mail: kopernik@agh.edu.pl

Received: August 8th, 2011
Accepted for publication: March 26th, 2012

was developed in the Programme – POLVAD_EXT and is shown in figure 1. The construction presented is 157 mm in length, 56 mm in width and 51 mm in height. The basic hydrodynamic parameters of POLVAD_EXT are [3]: average flow 2–5 dm^3/min, ventricular stroke volume 80–90 cm^3, typical loading pressure in outlet connector 90–160 mmHg, loading pressure in inlet connector 15 mmHg and pressure rise less than 4700 mmHg/s. The POLVADs are used to keep patients alive with a good quality of life while they wait for a heart transplantation which is known as a "bridge to transplantation". However, they are sometimes used as destination therapy and sometimes as a bridge to recovery.

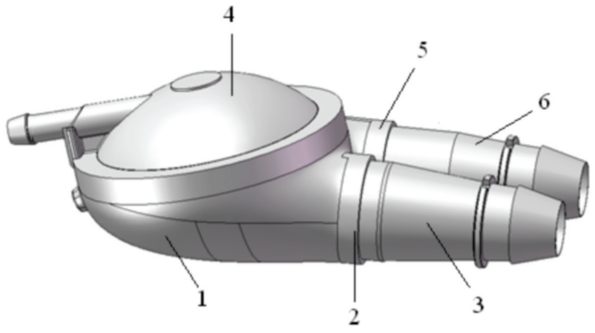

Fig. 1. CAD model of the POLVAD_EXT:
1 – blood chamber, 2 – inlet valve, 3 – inlet connector,
4 – pneumatic chamber, 5 – outlet valve, 6 – outlet connector

Thus, the developed construction of POLVAD_EXT needs optimization with respect to parameters of geometry, material models of polymer and deposited coating. The authors proposed a numerical model of POLVAD [8] composed of macro- and micromodel. This approach allows multiscale analysis of stress and strain states for different versions of POLVADs [9] and investigation [10] of parameters for their construction.

The goal of the present paper is to develop a multiscale model of blood chamber of POLVAD_EXT working under blood pressure at different temperatures and to verify distributions of strain and displacement computed on external surfaces of blood chamber by comparison with the distributions of strain and displacement measured and calculated in digital image correlation (DIC).

The second goal of the present work is to show the difference between stress and strain computed on internal and external surfaces of the blood chamber of POLVAD and POLVAD_EXT. The experiment applied to validate the strain and displacement is limited to the external surface of the blood chamber. Therefore, it is justified to show the difference between results reached on these two surfaces in two versions of VADs.

2. Materials and methods

The multiscale model of POLVAD_EXT needs experimental verification. Therefore, two experiments were performed in the Foundation of Cardiac Surgery Development in Zabrze, Poland:

- Tension test – determination of material properties of polymer for the POLVAD_EXT,
- DIC [11] – determination of deformation of external surface of the POLVAD_EXT.

The first experiment was static uniaxial tension test carried out for 12 specimens of polymer Chronoflex C 55D at two temperatures (21 °C and 38 °C) and stretched with velocity of 10 mm/min. Dimensions of specimens were: thickness 4.09 ± 0.04 mm, width 6.11 ± 0.07 mm and length 35 mm. The specimens were prepared by injection method and tested on MTS Criterion Single machine equipped with force sensor of 5 kN. The data registered was developed in MTS TestWorks™ software. Tests and calculations were performed according to ISO 527-2 and ASTM D 638 standards.

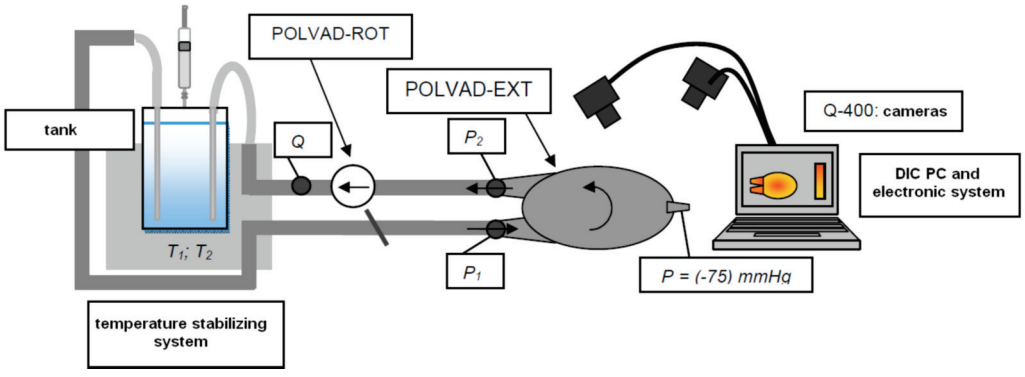

Fig. 2. Scheme of the DIC experiment

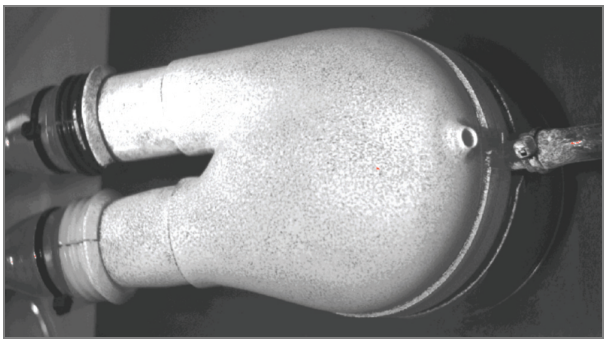

Fig. 3. Blood chamber of the POLVAD_EXT registered by one of the cameras in the DIC experiment

The second experiment was based on the idea of digital image correlation [11] used in analysis of the fields of deformation and displacement of material during loading. The following components were used in the experiment: the head Q-400 of Dantec Dynamics GmbH (Ulm, Germany) composed of two cameras CCD (1/1.8″, 1624 × 1234 pixels) in stereoscopic system, light sources (LED) and ISTRA 4D software installed on laptop. The POLVAD_EXT examined was connected to drains with water bath heating the water. The constant flow of water (0.1 dm^3/min) was provided by the use of a centrifugal pump. The pressure was registered in the blood chamber of POLVAD_EXT. A scheme of the experiment proposed is shown in figure 2. The POLVAD_EXT was loaded in steps of pressure: 80, 120, 180, 220, 280 mmHg, and in steps of underpressure: –25, –45, –75 mmHg. The subsequent images were taken after stabilization of pressure on a set level and the example of image taken by one of the cameras is presented in figure 3. The measurements were performed at two temperatures (25 °C and 37 °C).

3. Twoscale numerical model

A twoscale model was considered: a macromodel of blood chamber of the POLVAD_EXT and a micromodel of a TiN nanocoating deposited on a polymer. The problem in a microscale was solved for a representative volume element (RVE). The parameters of the model, corresponding to the macroscale are the macroparameters and will be denoted by a superscript *M*, for example, macrostress $-\sigma^M$. On the contrary, the parameters corresponding to the RVE in a microscale are the microparameters and will be denoted by a superscript *m*, for example, microstress $-\sigma^m$. All average values of symbols referring to the RVE will be denoted by an upper bar, for example, a mean microstress $-\overline{\sigma}^m$. In the twoscale model, the macrostress σ_{ij}^M and macrostrain ε_{ij}^M tensors corresponding to a certain point X^M in the macromodel can be evaluated directly by the average volume of a microstress σ_{ij}^m and a microstrain ε_{ij}^m over RVE.

3.1. Macroscale

The macroscale boundary problem is formulated for the theory of a nonlinear elasticity and the distribution of displacements U_i^M. The approach proposed describes deformation of the chamber of POLVAD_EXT under blood pressure if:

- stresses are related to strains by nonlinear equations (according to the nonlinear theory of elasticity),
- strain disappears in unloading conditions.

The nonlinearity in an elastic deformation process of blood chamber is a result of:

- nonlinear mechanical properties of a polyurethane,
- deposition and growth processes of the nanocoatings which cause the residual stress.

The problem of the blood chamber deformation in macroscale is considered as a 3D solution. Thus, the defined boundary problem of the theory of nonlinear elasticity is composed of the groups of equations described in [6], [7]. In the nonlinear zone of deformation, the effective stress σ_i^M is a function of deformation ε_i^M and temperature *t*. The effective Young's modulus is used instead of Young's modulus in each iteration.

The problems of convergence in a non-linear task in macroscale are solved in the present work by an iterative method. The effective Young's modulus E_{eff} is calculated in the next iteration $k + 1$ by the following formula:

$$E_{eff}^{M(k+1)} = \frac{\sigma_i^{M(k)}}{\varepsilon_i^{M(k)}} \tag{1}$$

where:

$E_{eff}^{M(k+1)}$ – the effective Young's modulus in the next iteration,

$\sigma_i^{M(k)}$ and $\varepsilon_i^{M(k)}$ – effective stress and effective strain in current iteration,

k – number of iterations.

The error of the effective Young's modulus δ is calculated by applying the formula:

$$\delta = \frac{E_{eff}^{M(k)} - E_{eff}^{M(k+1)}}{E_{eff}^{M(k)}} \tag{2}$$

where:

$E_{eff}^{M(k)}$ – the effective Young's modulus in the previous iteration,

$E_{eff}^{M(k+1)}$ – a value calculated by using equation (1).

The relation $\sigma_i^M(\varepsilon_i^M, t)$ is determined in tensile tests.

The components of stiffness matrix $[K]$ and complete load vector $\{F\}$ are written in the following forms:

$$[K_e^M] = \int_{V_e} [B]^T [D^M][B] dV , \tag{3}$$

$$\{F_e^M\} = -\int_{S_e} [N]^T \{p^M\} dS , \tag{4}$$

where:

S – contact surface,

$\{p^M\}$ – pressure inside blood chamber of POLVAD_EXT,

$[B]$ – matrix containing derivatives of shape functions,

$[D^M]$ – matrix containing the appropriate material properties (E^M, v^M),

$[N]$ – matrix of shape functions of a finite element,

V – volume,

V_e – volume of current finite element e,

S_e – contact surface between current element and blood chamber of POLVAD_EXT.

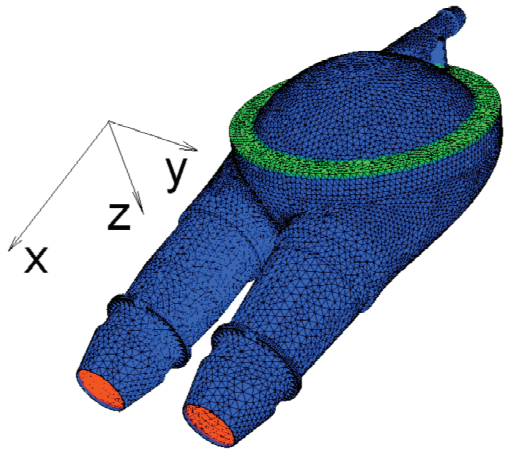

Fig. 4. Boundary conditions in a macromodel of the POLVAD_EXT and orientation of a coordinate system (red – pressure, green – fixed surface, blue – free surface)

The tetrahedron element with a five-point scheme of integration is used in the macromodel of POLVAD_EXT. The boundary conditions applied in the macromodel of POLVAD_EXT are in accordance with settings in DIC experiment (figure 4) and are as follows:

- a distribution of blood pressure $p^M = p = 37$ kPa on the inner surface of the blood chamber,
- fixed surfaces in the outer upper part of the blood chamber (no displacement in Z direction),
- not fixed surfaces in the outer part of the blood chamber (no loading).

3.2. Microscale

The analysis of strain distributions on inner surface of the blood chamber in the macroscale FEM model is used to determine areas with the biggest tendency to failure. The FE elements with the maximum values of a strain and stress located between two connectors on the inner surface of blood chamber are automatically selected by the authors' FE program and investigated in the microscale model. The strain reached during loading in macromodel is introduced into FEM micromodel as input data. The proposed microscale model of a wall of the POLVAD_EXT is described below.

The representative volume element is composed of a polymer and a TiN nanocoating. The parameters of an elastic-plastic material model of TiN were identified in the authors' earlier work [5]. Thus, a nonlinearity of mechanical properties between TiN coating and polymer exists. Considering such phenomena as elastic as well as an elastic-plastic deformation and unloading process, the boundary problem in the microscale is solved by the FEM micromodel. Assuming the elastic-plastic or nonlinear elastic material model is justified, the initial stress $\{\sigma_{0\,res}\}$ in TiN nanocoating is taken into account in the FEM formulation. The relation between stresses and strains is written using the matrix (vector) definition:

$$\{\sigma^m\} = [D^m]\{\varepsilon^m\} - \{\sigma_{0res}^m\} \tag{5}$$

where:

$\{\sigma_{0res}^m\}$ – residual stresses,

$\{\sigma^m\}$ and $\{\varepsilon^m\}$ – stress and strain tensors in a vector format.

The variational principle of the nonlinear elastic and elastic-plastic theory leads to the following functional form for a finite element e in the RVE:

$$W = \int_{V_e} \frac{1}{2} \{U^m\}^T [B]^T [D^m][B]\{U^m\} dV$$

$$-\int_{V_e}\{U^m\}^T[B]^T\{\overline{\sigma}^m_{0res}\}dV$$

$$-\int_{S_e}\{U^m\}^T[\overline{N}]^T\{p^m\}dS \qquad (6)$$

where:

$\{U^m\}$ – vector of displacement in nodes of elements,

$\overline{\sigma}^m_{0res}$ – experimental value of residual stress in current finite element *e*. The value of $\overline{\sigma}^m_{0res}$ in TiN nanocoating is based on results obtained in work [5].

The effective Young's modulus (equation (1)) is used instead of Young's modulus in an elastic zone for linearization of the functional (equation (6)) for a nonlinear problem:

$$E^m_{eff}=\frac{\sigma^m_i}{\varepsilon^m_i}. \qquad (7)$$

The stiffness matrix $[K]$ (equation (3)) and load vector $\{F\}$ are written according to the forms:

$$[K^m_e]=\int_{V_e}[B]^T[D^m][B]dV, \qquad (8)$$

$$\{F^m_e\}=-\int_{V_e}\{U^m\}^T[B]^T\{\overline{\sigma}^m_{res}\}dV-\int_{S}[\overline{N}]^T\{p^m\}dS. \qquad (9)$$

The residual stress in TiN nanocoating must be evaluated before the simulation of loading (figure 5). After implementation of $\overline{\sigma}_{0\,res}$, the simulations of loading and unloading stages in a microscale are possible. In the present work, the experimental residual stress is interpreted as a mean stress and is localized in the TiN nanocoating.

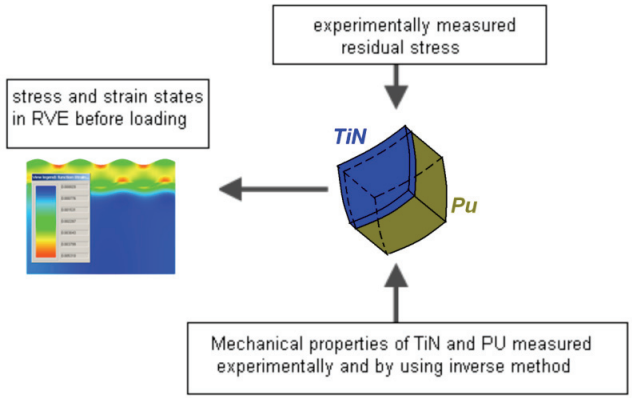

Fig. 5. Scheme of residual stress modelling

The representative volume element (RVE) is an intermediate scale between the micro- and macroscales. The following boundary conditions can be imposed on the surface of RVE:

- Kinematic boundary conditions:

$$U^m_i=\varepsilon^M_{ij}x_i. \qquad (10)$$

- Static boundary conditions:

$$n_i\sigma^m_{ij}=n_i\sigma^M_{ij}. \qquad (11)$$

The average stress inside the RVE is equal to σ^M_{ij}.

- Periodic boundary conditions: a displacement component is imposed perpendicularly to the side of the RVE, but parallel to the side and they are let free.

The periodic boundary conditions (PBC) are used in the parallel direction of the surface of blood chamber and the static boundary conditions are applied in the direction of the blood pressure. Considering the TiN nanocoating, the following modification of the PBC is proposed. The deformation tensor is taken from the macroscale in modelling the boundary conditions of the RVE (figure 6). The direction of normal to the surface of RVE for TiN nanocoating corresponds to the direction of a hydrostatic pressure p (blood pressure p^m). Therefore, shear stresses and strains are not present on this surface and stress p is one of the principal stresses of the stress tensor. Thus, the solution in a main coordinate system is found. The principal strains can be used as boundary conditions. Each side of the RVE is a symmetry plane with these boundary conditions, because the shear stresses and strains are zero. The $2^1/_2$ boundary problem is considered and 4-node finite elements are used. The strain ε^M_2 (second principal strain of strain tensor) is introduced into the microscale as a constant. Therefore, the 3D boundary problem of the RVE deformation is transformed to the 2D plane strain problem with the current value of ε^M_2. The principal strain ε^M_1 and pressure $p^M=p^m=p$ are also used in the model of the RVE.

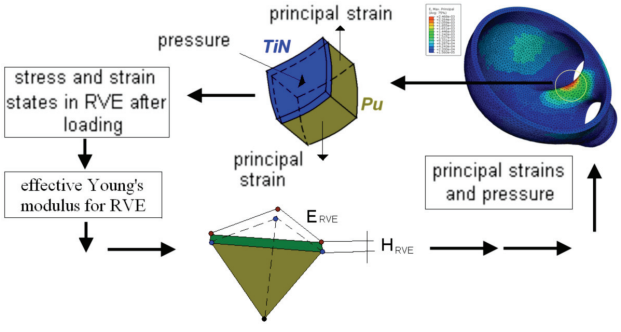

Fig. 6. Scheme of active loading modelling

4. Results and discussion

4.1. Material model of polymer

The first step of numerical analysis was dedicated to identification of parameters in a material model of a polymer based on the tension test data. The material model selected for the polymer is as follows:

$$\sigma = A\varepsilon^{n_1} \exp(n_2\varepsilon)\exp(-n_3 t) \qquad (12)$$

where:

A, n_1, n_2 and n_3 – parameters,
t – temperature,
ε – strain,
σ – stress.

The parameters of material model of the polymer are shown in table 1. The raw tension test data and results of approximation are presented in figure 7. The results of tension test obtained for ChronoFlex C 55D at 21 °C and 37 °C show that strain changes twice at these two temperatures. Stain 0.05 corresponds to stress 2.1 MPa and 4.4 MPa. Thus, it is necessary to consider changes of temperature of the material of the blood chamber wall in all numerical models. Based on the identified material model of polymer the approximation was made for the results of the tension test data obtained at 25 °C (figure 7). The material model of polymer at 25 °C will be introduced into macromodel of the blood chamber of POLVAD_EXT as input data.

Table 1. Parameters identified in material model of polymer

Parameters	Value
A	104.54 MPa
n_1	0.75
n_2	–3.37
n_3	0.04

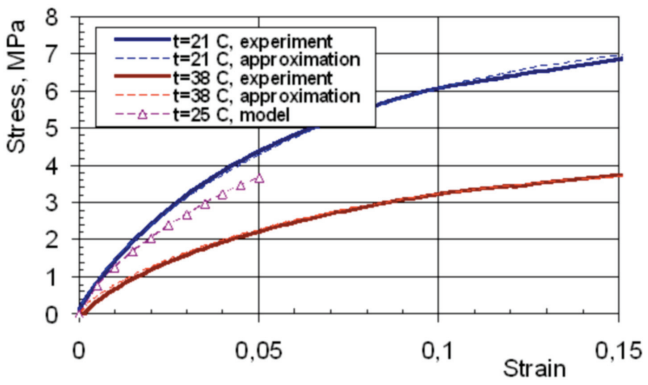

Fig. 7. Stress-strain curves for the ChronoFlex C 55D

4.2. FEM model and DIC experiment

The next step was to apply the boundary conditions in a macromodel of the blood chamber as they were in the DIC experiment. A FEM mesh of blood chamber with boundary conditions and an orientation of a coordinate system are shown in figure 4. Then, the simulations were performed for blood chamber of the POLVAD_EXT made of ChronoFlex C 55D under a pressure of 37 kPa and at a temperature of 25 °C. The results of numerical tests obtained on the external surface of FEM macromodel were compared with the DIC results (figures 8–11). Two regions are distinguished on the surface of blood chamber considering distribution of displacement in X direction (figure 8): the region which is closer to the point where two connectors are mounted, and the region which is closer to the point of the VAD's pneumatic control. The big difference of displacement in X direction for these two regions (two maxima) is visible on the external surfaces of blood chamber in experiment and in simulation. Therefore, a comparison of the distribution of displacement in X direction (figure 8) shows acceptable qualitative coincidence between experimental and numerical results. The observed quantitative coincidence is worse, which means that the value of difference between displacements in X direction for the two regions distinguished is not exactly the same in simulation and in experiment.

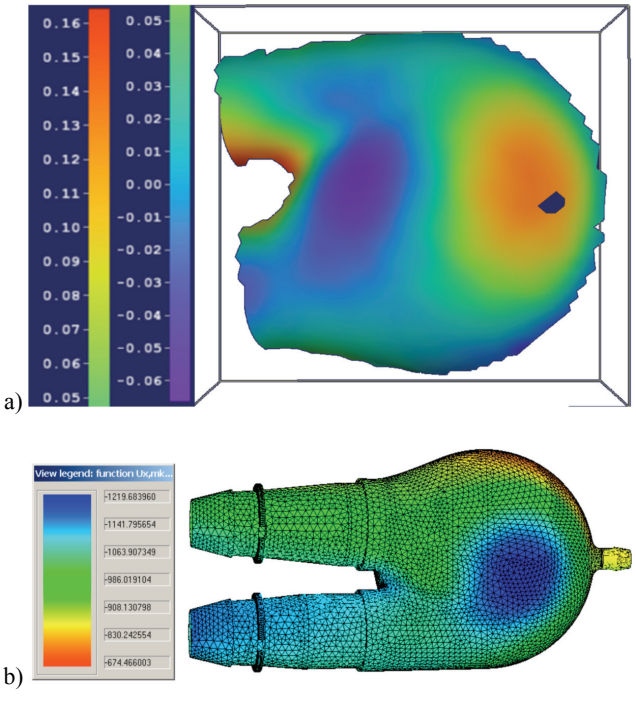

Fig. 8. Displacement U_x: (a) experiment, mm, (b) FEM simulation, μm

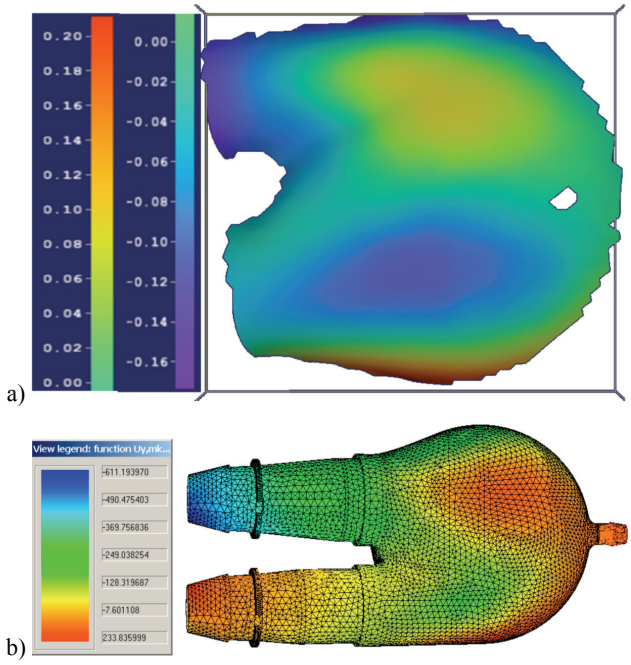

Fig. 9. Displacement U_y:
(a) experiment, mm, (b) FEM simulation, μm

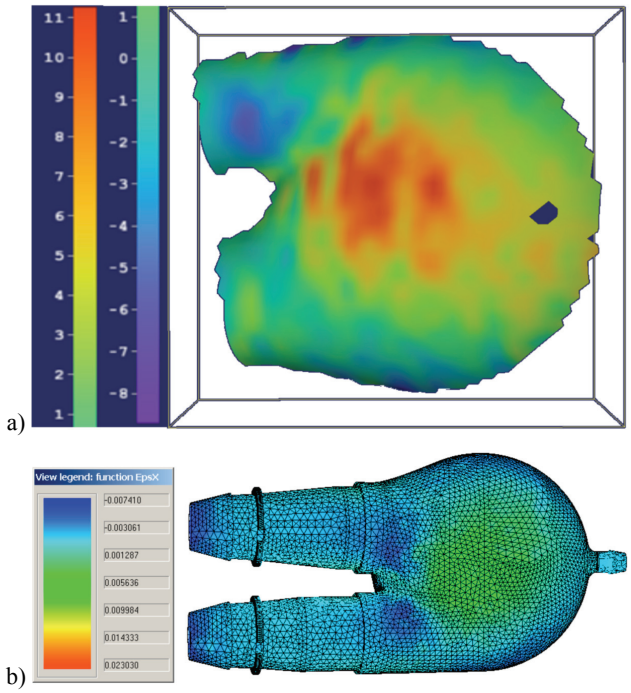

Fig. 10. Distribution of strain ε_x:
(a) experiment, mm/m, (b) FEM simulation

A comparison of the distributions of displacements computed in *Y* direction (figure 9) gives acceptable qualitative and quantitative coincidence between experimental and numerical results. The maxima of displacements on external surface of blood chamber of POLVAD_EXT are 1.2 mm in experiment and 1.154 mm in simulation in *Z* direction. These values

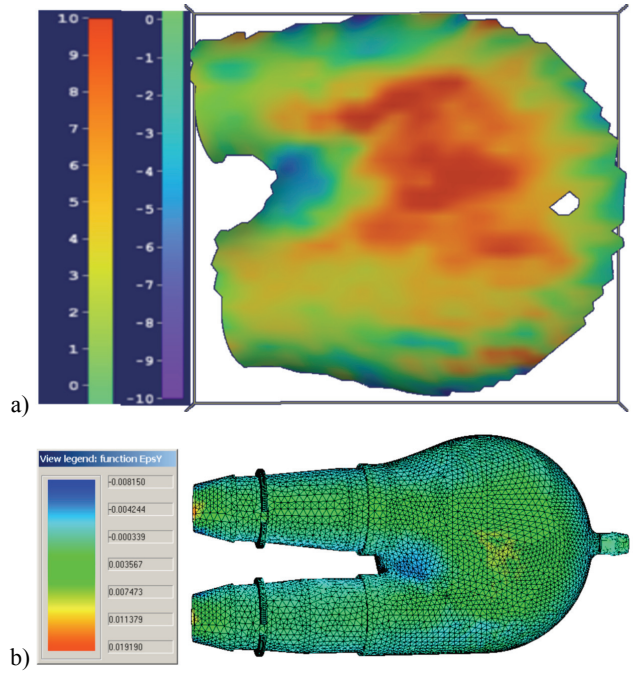

Fig. 11. Distribution of strain ε_y:
(a) experiment, mm/m, (b) FEM simulation

are located on the external surface at the central point of the blood chamber.

After this analysis, the strains obtained on external surface of the FEM macromodel and in the DIC experiment were compared (figures 10 and 11). It should be noted that strains are more reliable than displacements, which may be disturbed by movements of the blood chamber difficult to be completely eliminated during the experiment. A comparison of experimental and numerical data for distributions of strains in *X* and *Y* directions indicates a good quantitative coincidence between results, but the qualitative comparison gives a little worse coincidence which is caused by some irregularities in distributions of experimental data. The maximum of strain (0.01) is observed for the POLVAD_EXT on the external surface in the DIC experiment at the central point of the blood chamber. The same result (strain 0.01) is computed for the FEM macromodel at the central point of the blood chamber.

4.3. External and internal surfaces of POLVAD and POLVAD_EXT

The acceptable difference between experiment and numerical simulation was a basis for comparative analysis of both versions of blood chambers (POLVAD and POLVAD_EXT) in numerical simulation. The DIC experiment allows limited verifica-

tion, because only the data obtained on external surface of the blood chamber can be analyzed. Thus, a comparison of results computed in the macromodel on external and internal surfaces of the two versions of blood chambers (POLVAD and POLVAD_EXT; made of a ChronoFlex C 55D and under a pressure of 37 kPa and at 25 °C) was made. Distributions of effective strains and stresses on external and internal surfaces of the blood chamber of POLVAD are shown in figures 12 and 13, and those of the POLVAD_EXT are shown in figures 14 and 15. The comparison of results computed in external and internal surfaces of the blood chambers of POLVAD and POLVAD_EXT shows that the values of effective strains and stresses on external surface are smaller than those on internal surface. This observation is in accordance with predictions, because the loadings are set to the internal surfaces. The maximum value of strain (0.027) is computed in internal surface of the blood chamber of POLVAD in the FE elements between two connectors. The strains and stresses are much smaller in a construction of the POLVAD_EXT than in the POLVAD and their distributions are more homogeneous. Therefore, the POLVAD_EXT is considered a better construction. The maximum values of stresses and strain are computed in the two blood chambers in a region between two connectors. This is the region in which a fracture of the blood chamber material may occur.

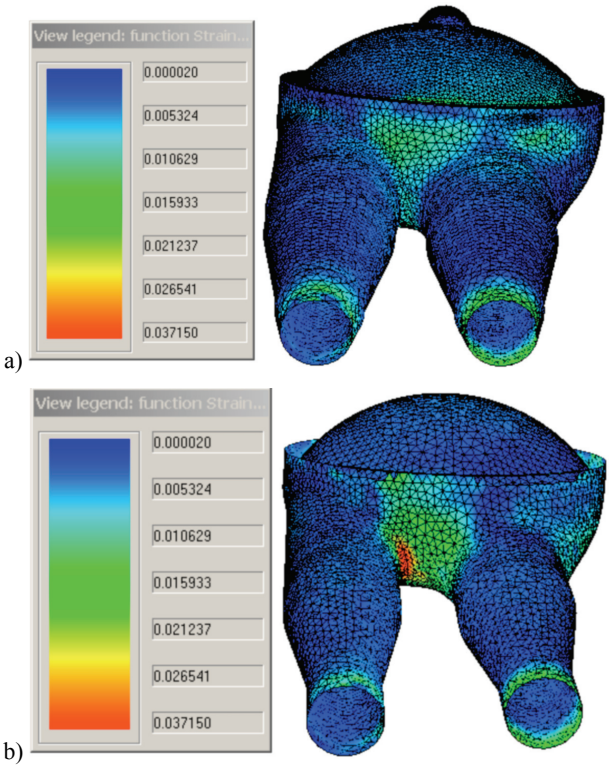

Fig. 12. Distribution of effective strain on external (a) and internal (b) surfaces of the POLVAD

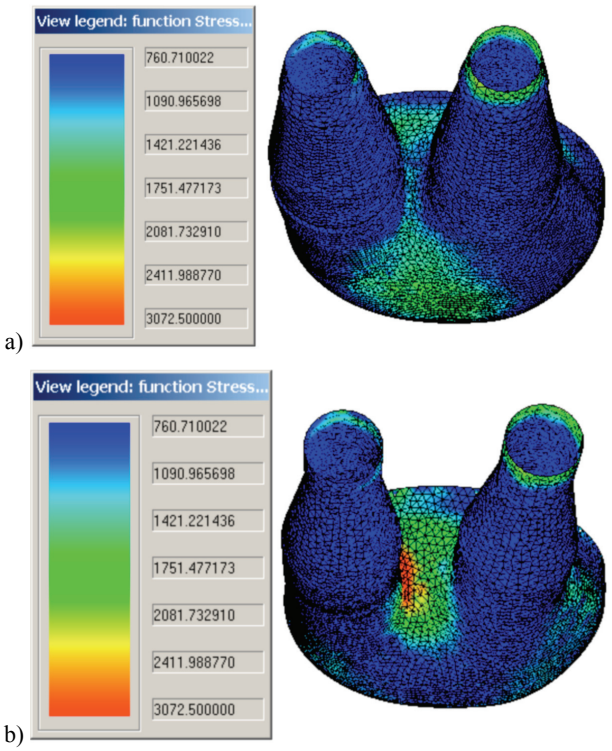

Fig. 13. Distribution of effective stress on external (a) and internal (b) surfaces of the POLVAD

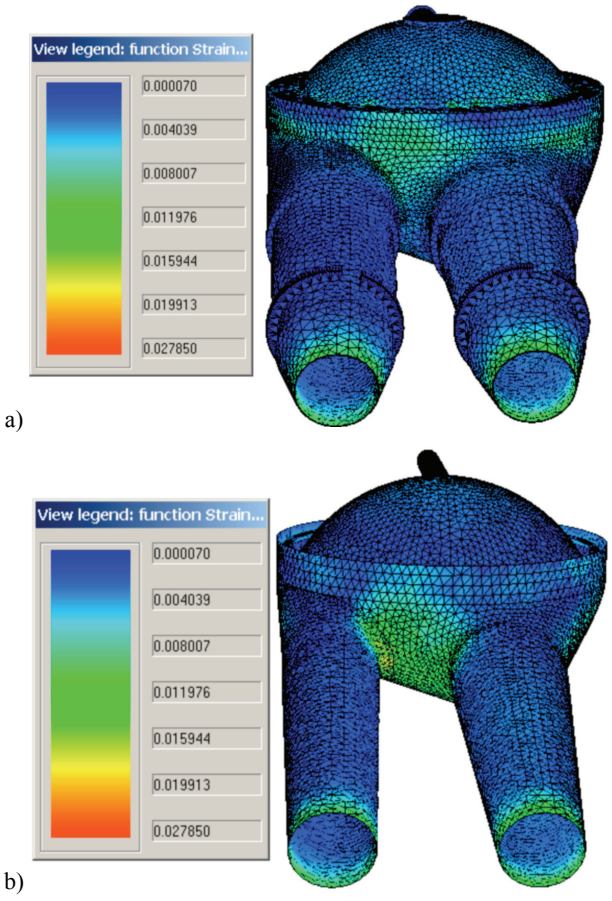

Fig. 14. Distribution of effective strain on external (a) and internal (b) surfaces of the POLVAD_EXT

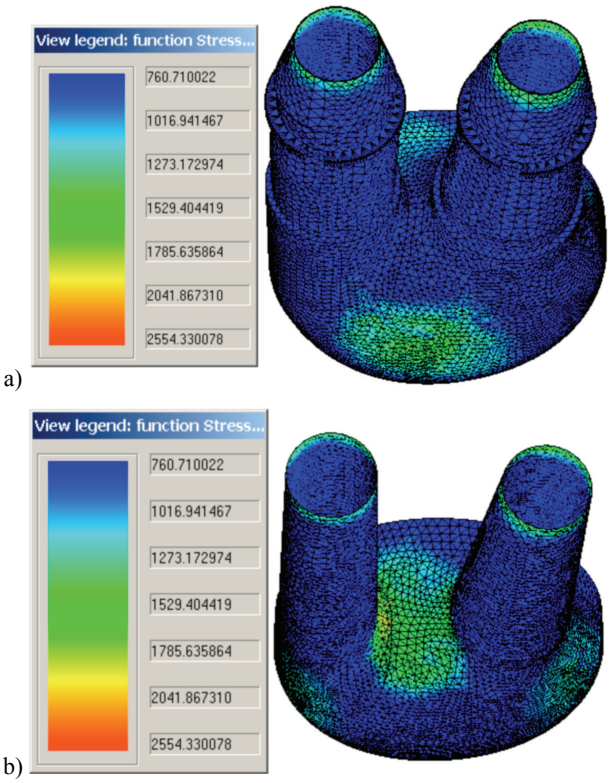

Fig. 15. Distribution of effective stress on external (a) and internal (b) surfaces of the POLVAD_EXT

5. Conclusions

• Polymer applied in the POLVADs is sensitive to changes of temperature and this observation should be considered in numerical models.

• A comparison of experimental and numerical strains and displacements obtained on external surfaces of the blood chamber in loaded POLVAD_EXT shows acceptable coincidence. The developed FEM macromodel of POLVAD_EXT and computer program allow simulation and optimization of different constructions of VADs in a macro- and a microscale.

• A comparison of two surfaces (external and internal) in two versions of blood chambers (POLVAD and POLVAD_EXT) in numerical analysis shows that the POLVAD_EXT construction is better with respect to the character of distributions of strain and stress, as well as their smaller values. The maximum values of computed parameters are located in the region between the connectors. The internal surfaces of the blood chambers have bigger values of strain and stress due to setting the loading directly on them.

Acknowledgements

Financial support of the MNiSzW, projects 08/WK/P02/0001/SPB–PSS/2008 and 2011/01/D/ST8/04087, is acknowledged.

References

[1] EBNER R., LACKNER J.M., WALDHAUSER W., MAJOR R., CZARNOWSKA E., KUSTOSZ R., LACKI P., MAJOR B., *Biocompatibile TiN-based novel nanocrystalline films*, Bulletin of the Polish Academy of Sciences, Technical Sciences, 2006, 54, 167–173.

[2] FRASER K.H., TASKIN M.E., GRIFFITH B.P., WU Z.J., *The use of computational fluid dynamics in the development of ventricular assist devices*, Med. Eng. Phys., 2011, 33, 263–280.

[3] GAWLIKOWSKI M., PUSTELNY T., KUSTOSZ R., *The physical parameters estimation of physiologically worked heart prosthesis*, Journal de Physique, 2006, 137, 73–78.

[4] GREGORY S.D., TIMMS D., GADDUM N., MASON D.G., FRASER J.F., *Biventricular Assist Devices: A Technical Review*, Ann. Biomed. Eng., 2011, 39, 2313–2328.

[5] KOPERNIK M., MILENIN A., MAJOR R., LACKNER J.M., *Identification of material model of TiN using numerical simulation of nanoindentation test*, Materials Science and Technology, 2011, 27, 604–616.

[6] MILENIN A., *Theoretical analysis of the stress-strain state in the region of the inclusion of second phase under plastic deformation of two-phase materials*, Russian Metallurgy, 1995, 2, 97–103.

[7] MILENIN A., *Bases of finite element method*, Akademia Górniczo-Hutnicza, Kraków, 2010.

[8] MILENIN A., KOPERNIK M., *The multiscale FEM model of artificial heart chamber composed of nanocoatings*, Acta of Bioengineering and Biomechanics, 2009, 11, 13–20.

[9] MILENIN A., KOPERNIK M., *Comparative analysis of ventricle assist devices POLVAD and POLVAD_EXT based on multiscale FEM model*, Acta of Bioengineering and Biomechanics, 2011, 13/2, 13–23.

[10] MILENIN A., KOPERNIK M., *Microscale analysis of strain-stress state for TiN nanocoating of POLVAD and POLVAD_EXT*, Acta of Bioengineering and Biomechanics, 2011, 13/4, 11–19.

[11] ORTEU J.J., *3-D computer vision in experimental mechanics*, Optics and Lasers in Engineering, 2009, 47, 282–291.

[12] PAN W., FEDOSOV D.A., CASWELL B., KARNIADAKIS G.E., *Predicting dynamics and rheology of blood flow: A comparative study of multiscale and low-dimensional models of red blood cells*, Microvasc. Res., 2011, 82, 163–170.

[13] SARNA J., KUSTOSZ R., MAJOR R., LACKNER J.M., MAJOR B., *Polish Artificial Heart – new coatings, technology, diagnostics*, Bull. Pol. Acad. Tech., 2010, 58, 329–335.

[14] YAMAGUCHI T., ISHIKAWA T., IMAI Y., MATSUKI N., XENOS M., DENG Y., BLUESTEIN D., *Particle-Based Methods for Multiscale Modeling of Blood Flow in the Circulation and in Devices: Challenges and Future Directions*, Ann. Biomed. Eng., 2010, 38, 1225–1235.